Pan-american Association of Computational Interdisciplinary Sciences

Journal of Computational Interdisciplinary Sciences (2011) 2(2): 79-86

Printed version ISSN 1983-8409 / Online version ISSN 2177-8833
http://epacis.net
doi: 10.6062/jcis.2011.02.02.0034

Multicanonical simulation and trapping due to high free-energy barriers in an Ising model for ultrathin magnetic films

Leandro G. Rizzi and Nelson A. Alves

Manuscript received on October 20, 2010 / accepted on August 15, 2011

ABSTRACT

Several studies to determine the nature of the thermodynamic phase transitions for an Ising model for ultrathin magnetic films have been reported in recent years. No conclusive results have been obtained yet, because the simulation with conventional Monte Carlo methods is slowed down by long relaxation times due to the suppression of tunneling events through free-energy barriers. In this paper we study the Ising model with dipolar interactions in two dimensions with an generalized-ensemble algorithm to address this problem. Herein, the multicanonical algorithm has been implemented in this study because it systematically explores energy configurations and enhances the rate of tunneling events. The success of a simulation depends on how often the algorithm explores the energy range between two extremal values. Our results indicate a limitation of the multicanonical algorithm in estimating the density of states for this model because the algorithm does not satisfactorily circumvent the problem of high free-energy barriers in the energy region where the nematic phase takes place.

Keywords: computational physics and chemistry, multicanonical algorithm, dipolar Ising model, free-energy barrier.

1 INTRODUCTION

Monte Carlo methods are commonly employed in distinct knowledge areas such as Chemistry, Biology, Astronomy, Physics, Medicine, and Social and Economic Sciences. In Physics, one of the main issues of Monte Carlo (MC) methods consists in obtaining efficient sampling of relevant configurations of models in Statistical Physics. An important task in this field is the description of the critical behavior of thermodynamic systems. However, this description is hampered by the critical slowing down [1]. This is even worse with respect to thermodynamic first-order phase transitions because the interfacial free-energy suppresses tunneling events between the macroscopic phases of the system. This suppression further decreases the performance of conventional simulations as the system size increases. Thus, an important issue is how many measurements are needed to get a reasonable sampling configurations. Nonlocal cluster algorithms [2, 3, 4] have been designed to eliminate this critical slowing down, but they are in essence restricted to spin systems with nearest-neighbor interactions. For general purposes, the generalized-ensemble techniques [5] present a far more efficient way to overcome free-energy barriers, thus improving the sampling performance.

In this paper the performance of the multicanonical algorithm (MUCA) for an Ising-like spin system in two dimensions (2D) has been studied. The MUCA has been successfully applied to many complex problems as 2D and 3D spin glass systems [6, 7], $SU(3)$ gauge theory [8, 9] and in simulations of peptides to explore the protein folding problem [10]. In principle, an Ising-like spin system could be considered a simple system, but it

Correspondence to: Leandro G. Rizzi
Departamento de Física, FFCLRP, Universidade de São Paulo, Avenida Bandeirantes 3900, 14040-901 Ribeirão Preto, SP, Brazil.
E-mails: lerizzi@usp.br / alves@ffclrp.usp.br

becomes complex when long-range dipolar interactions are added. The simulation of such system with conventional MC methods is slowed down by highly correlated configurations generated by these algorithms. To be precise, we consider the 2D Ising model with competitive nearest-neighbor ferromagnetic and long-range dipolar interactions. The Hamiltonian is defined on a lattice with $N = L^2$ sites occupied by Ising spins $\sigma_i = \pm 1$,

$$\mathcal{H} = -\delta \sum_{<i,j>} \sigma_i \sigma_j + \sum_{i<j} \frac{\sigma_i \sigma_j}{r_{ij}^3}, \qquad (1)$$

where $\delta = J/g$ is the ratio between the ferromagnetic exchange interaction ($J > 0$) and the dipolar antiferromagnetic interaction of strength $g > 0$, and r_{ij} is the distance between distinct pairs of lattice spins i and j.

This model has been used to describe thermodynamic properties of ultrathin magnetic films [11]. The magnetization in these films is characterized by different patterns of magnetic domains, which have been observed, for example in ultrathin ferromagnetic films of Fe on Cu [12]. The presence of competing long-range and short-range interactions gives rise to the frustration phenomenon and thus, to a rich phase diagram [13]. The usual ferromagnetic ground-state of the 2D Ising model changes to a series of alternating striped spin configurations. Each stripe corresponds to a pattern of upward or downward spins, and its width h increases with δ.

One observes two different scenarios for this model in the $T - \delta$ phase diagram according to the patterns of magnetic domains that may emerge as a consequence of the disordering of the striped ground state. In the first scenario, the system experiments one phase transition from the striped phase to the tetragonal phase as the temperature rises. The loss of ordering is explained in terms of topological defects, such as dislocations and disclinations [11]. Thus, a mechanism for this stripe melting is based on topological defects, which might penetrate the system and induce geometrical phase transitions. For a square lattice, this symmetry-breaking phase is referred to as the tetragonal phase [14, 15] and is characterized by magnetic domains that are no longer aligned along a common direction of the lattice.

The second scenario is characterized by a two-step melting process where a nematic phase appears in between the striped and the tetragonal phases [16]. Since the phases are analogous to those observed in liquid cristals, the terminology is maintained. The new intermediary phase still keeps the overall orientational order, but it is less symmetric when compared with the striped phase.

Recently, we investigated the second scenario in the region for coupling $\delta = 2$ with the Metropolis algorithm and using the multiple histogram analysis [17]. This analysis consisted of the reweighting technique applied to multiple MC simulations to broad the energy range sampled. The multiple histogram analysis of the energy density distributions $P(E)$ revealed a strong first-order nature for the striped-nematic phase transition. However, our finite-size scaling (FSS) analysis of the specific heat and susceptibility did not support such picture. It has been pointed out that this transition also resembles the Kosterlitz-Thouless like phase transition because the specific heat tends to saturate as a function of the lattice size [16]. Controversial results are also obtained for the nematic-tetragonal phase transition. Again, the first-order nature was suggested by the energy density distributions obtained via multiple histogram analysis, but the FSS analysis of the specific heat did not discard the second-order nature for this phase transition [17]. The authors in [16] argue that the nematic-tetragonal phase transition has the first-order character, but their arguments are also based on results from simulations with local update algorithm. We have also found that the response functions specific heat and susceptibility have strong finite-size effects, which frustrate any convincing evaluation of the critical exponents from simple FSS analysis. Therefore, the true phenomenology of this model, which corresponds to a two-step melting process, is observed for large lattice sizes only. It has been reported very long-lived states near the low temperature phase transition [18], and evaluation of the autocorrelation times yields large values for the critical dynamical exponent z [17]. Moreover, the numerical simulations are very CPU time consuming because of the dipole interaction term.

The generalized-ensemble algorithms are an alternative to the conventional MC methods because they lead to a far more efficient sampling. In this paper, results of the standard implementation of the multicanonical algorithm [19, 20, 21] for the coupling $\delta = 2$ are discussed. The implementation corresponds to a protocol where the multicanonical weights are updated recursively at every n_s MC sweeps.

The paper is organized as follows. In Section 2 the theoretical concepts of the multicanonical method and the reweighting data procedure are reviewed. Some technical details and the main results regarding the performance of our numerical tests are presented in Section 3. Our conclusions are summarized in Section 4.

2 MULTICANONICAL ALGORITHM

The conventional Metropolis algorithm is defined by the Boltzmann weight $w(E) = e^{-\beta E}$, where $\beta = 1/T$ with the

Boltzmann constant $k_B = 1$. Significant improvement has been achieved with the generalized algorithms, which are based on non-Boltzmann sampling weight factors. These algorithms try to enhance the number of tunneling events, thereby allowing for more efficient sampling of states.

Let $w(E)$ be a MC weight where $E = \mathcal{H}(\{\sigma_i\})$ is the energy of a state given by the specific set of general coordinates $\{\sigma_i\}$, with $i = 1, \ldots, N$, for N degrees of freedom. As usual, a new state with energy E' is proposed and accepted with probability given by

$$p(E \to E') = \min\left[1, \frac{w(E')}{w(E)}\right]. \qquad (2)$$

With a convenient weight $w(E)$ and for sufficiently long simulation times, the configurational sampling produces the equilibrium energy histogram $H(E) = \Omega(E)w(E)$, where $\Omega(E)$ is an estimation of the density of states of the system.

One of such generalized algorithms is the MUCA, which defines weights that samples all the energies with the same probability and was proposed by Berg and Neuhaus in 1991 [19]. For a detailed description of the algorithm and references for its applications, see [20, 21]. For details of our actual implementation, see [21].

The method consists of sampling configurations with weight $w_{mu}(E) \simeq 1/\Omega(E)$. Therefore, the histogram $H(E) \propto \Omega(E)w_{mu}(E)$ is almost flat. If the Boltzmann entropy $S(E) = \ln \Omega(E)$ is considered, it is convenient to write the following parameterization $S(E) = b(E)E - a(E)$, where $a(E)$ and $b(E)$ are the multicanonical parameters. Thus, the multicanonical weight is given by $w_{mu}(E) = \exp[-b(E)E + a(E)]$, with the parameter $a(E)$ related to a multicanonical free-energy and $b(E)$ to the inverse of microcanonical temperature.

Since the weight $w_{mu}(E)$ is unknown *a priori*, we must proceed as follows. Firstly, the multicanonical parameters $a(E)$ and $b(E)$ from N_r recursion steps are obtained. Usually, the number N_r is defined *a posteriori* when the multicanonical parameters present some convergence. The nth recursion step is performed after the histogram $H_{mu}^{n-1}(E)$ is obtained from n_s MC sweeps according to the acceptance probability (2) and weight $w_{mu}^{n-1}(E)$.

The implementation of the multicanonical method requires the discretization of the energy. To this end, the labeled energies $E_m = E_0 + m\varepsilon$ are defined, where each energy is associated with an integer number $m = 0, \ldots, M$. All the energies in the interval $[E_m, E_{m+1}[$ are in the mth energy bin of size ε and contribute to the histogram $H_{mu}(E_m)$. The constant E_0 is defined as a reference energy near but below the ground-state energy.

Table 1 – Time in seconds for one sweep for different lattice sizes. These results are obtained in AMD Opteron 64bit machines with Dual Core 2.6 GHz processors and fortran90 language running on a Linux (Gentoo *release* 2006.0) platform.

L	time (s)
32	0.014895(2)
48	0.07621(1)
56	0.13262(2)
72	0.3873(5)

The recursion steps consist of updating the multicanonical parameters,

$$a^n(E_{m-1}) = a^n(E_m) + \left[b^n(E_{m-1}) - b^n(E_m)\right]E_m\,, \qquad (3)$$

$$\begin{aligned} b^n(E_m) &= b^{n-1}(E_m) \\ &+\left[\ln \hat{H}_{mu}^{n-1}(E_{m+1}) - \ln \hat{H}_{mu}^{n-1}(E_m)\right]/\varepsilon\,, \end{aligned} \qquad (4)$$

with $n = 1, \ldots, N_r$ and

$$\hat{H}_{mu}^{n}(E_m) = \max[h_0, H_{mu}^{n}(E_m)]\,,$$

with $0 < h_0 < 1$. It is convenient to compute the above recurrence relations with the initial conditions $a^0(E_m) = 0$ and small values for $b^0(E_m)$ if the simulation uses a hot-start initialization. As the multicanonical parameters are updated, the method samples configurations with lower energies.

The Ewald summation technique has been implemented (details can be found in [22]) to evaluate the dipole interaction term with periodic boundary conditions. Table 1 lists the CPU time estimates for one Monte Carlo sweep. This table shows that the CPU time as a function of the lattice size L scales as $L^{3.6}$.

Data production is obtained with further n_{meas} sweeps by using the last updated weight $w_{mu}^{n=N_r}(E)$. Afterwards, the desired canonical estimates for physical quantities A are evaluated by reweighting the collected data,

$$\overline{A(\beta)} = \frac{\sum_{k=1}^{n_{meas}} A_k \left[w_{mu}^{N_r}(E_k)\right]^{-1} \exp\left(-\beta E_k\right)}{\sum_{k=1}^{n_{meas}} \left[w_{mu}^{N_r}(E_k)\right]^{-1} \exp\left(-\beta E_k\right)}\,. \qquad (5)$$

An advantage of the reweighting procedure combined with multicanonical production is that one can obtain estimates for physical quantities at any temperature. This contrasts with the Metropolis algorithm, where the reweighting is restricted to a very narrow temperature range around the fixed temperature in the Boltzmann weight.

3 RESULTS AND DISCUSSION

All simulations were performed for $\delta = 2$ with $E_0 = -1.22L^2$ and the choice $M = 2L^2$, but it must be borne in mind that the value E_0 should be chosen according to the coupling δ. We emphasize that the constant E_0 is defined as a reference energy near but below the ground-state energy. One can evaluate the ground-state energies plotting Equation (1) *versus* δ for different striped spin configurations. For instance, for $\delta = 2$ the lowest energy configuration displays stripes of width $h = 2$ [23]. This configuration yields the ground-state energy $E_{GS} \sim -1.209$ per degree of freedom. Therefore, we found convenient to choose $E_0 = -1.22\,N$.

The convergence of multicanonical parameters was analyzed for lattice sizes $L = 32$, 48, and 56. We always started the MC runs from a disordered configuration and define the acceptance probabilities for spin updates based on the Metropolis scheme according to Equation (2) and initial multicanonical parameters $a^0(E_m) = 0$ and $b^0(E_m) = 0.02$ for all m.

The value $h_0 = 0.1$ was chosen in our simulations, but as discussed in [20] the specific numerical value is not relevant provided that $0 < h_0 < 1$. The statistics amounts to $n_s = 5 \times 10^4$ sweeps per recursion step. This number was decreased to $n_s = 2 \times 10^4$ sweeps in order to study the influence of the energy bin size ε and to explore the performance of the algorithm when one increases the frequency of multicanonical updates. This last study was carried out for lattice sizes $L = 48$ and 56.

Firstly, our study concerning the multicanonical parameters is presented for $L = 32$. Figure 1 shows the updated histogram $H_{mu}^{n-1}(E)$ and the multicanonical parameter $b^n(E)$ for $L = 32$ and $\varepsilon = 2$ at two different recursion steps. Figure 1(a) shows that the histogram does not contain appreciable energy measurements for $E/N \lesssim -1.15$. This is quite typical for recursion steps up to $n \sim 100$. Thus, the $b(E)$ determination exhibits a noisy behavior for energies $E/N \lesssim -1.15$. The multicanonical parameters had to be updated up to $n = 400$ to see some improvement in the $b(E)$ estimation around this energy, as depicted in Figure 1(d). A typical histogram $H_{mu}(E)$ for such large number of recursion steps is represented in Figure 1(c). The peak in $b(E)$ for $n = 400$ is at $E/N \sim -1.12$.

The microcanonical specific heat $C_v(E) = dE/dT$ can be rewritten as $C_v(E) = -[dS(E)/dE]^2/(d^2S/dE^2)$ [24]. Multicanonical relations connect the parameter $b(E)$ with the inverse of the microcanonical temperature. Therefore, the specific heat can be written in terms of $b(E)$ as

$$C_v(E) = -b(E)^2/[db(E)/dE]\,,$$

and the values E^* where $db(E)/dE|_{E^*} = 0$ signal divergences in $C_v(E)$. Therefore, two energy candidates where one can observe such divergence in C_v are at $E/N \sim -1.12$ and at a lower energy $E/N \sim -1.15$. Reference [17] identifies the canonical specific heat maximum at $E/N \sim -1.13$, which corresponds to $T \sim 0.7905(3)$. This behavior is reproduced in Figure 4(b). Thus, the canonical estimate [17] corresponds to an average energy of the above microcanonical estimates. Figure 1(c) reveals that the system was trapped in the lower energy phase, corresponding to the striped phase. In general, there is a suppression of configurations between the important energies $E/N \sim -1.15$ and -1.12.

Figure 2 exhibits our multicanonical study for $L = 48$. Here, a smaller energy bin $\varepsilon = 1$ was employed, so that more precise estimates for the derivative of $b(E)$ could be achieved. Figures 2(a) and 2(b) give results obtained after $n = 150$ recursion steps. The parameter $b(E)$ is very noisy for such number of recursion steps. In particular, the simulation at this stage produces histograms with energies in the striped phase mainly. In general, the simulation does not seem to explore the whole energy space, as one can observe in Figures 2(a), 2(c), and 2(e). Therefore, tunneling events are suppressed because of the free-energy barriers related to the striped-nematic and nematic-tetragonal phase transitions. Figure 2(f) shows that the number of multicanonical updates had to be raised to $n = 550$, in order to reduce the noise in $b(E)$ at the energy region where the peak appears. At this stage, our statistics amounts to 27.5×10^6 sweeps. The points where $db(E)/dE = 0$ correspond to the peaks and valleys in $b(E)$. The peaks are located at $E/N \sim -1.16$ and $E/N \sim -1.05$. The valleys are located at $E/N \sim -1.17$ and $E/N \sim -1.08$. The canonical estimates [17] for the maximum of C_v correspond to $E/N = -1.145$ and $E/N \sim -1.06$, respectively for the striped-nematic and nematic-tetragonal phase transitions. These values are in good agreement with the naive estimates from $b(E)$. It is also clear from Figure 2(f) that the estimates for $b(E)$ were improved for energies around $E/N = -1.16$, but we had to raise N_r to 550. In general, for $L = 48$ the histograms do not contain energies that would result from satisfactory round trips between the lower energy phase and the higher energy one.

Figure 3 corresponds to our tests for $L = 48$ and different

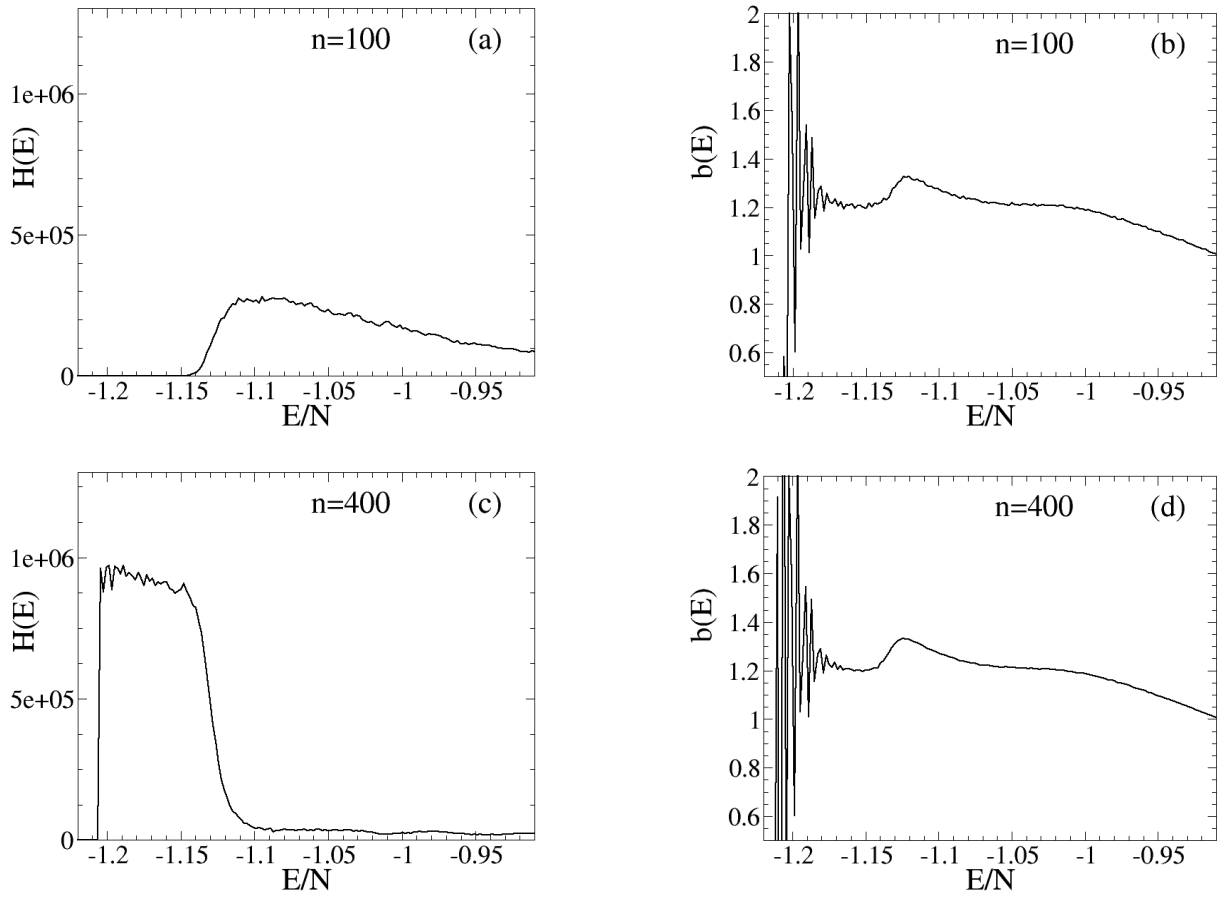

Figure 1 – Behavior of $H_{mu}^{n-1}(E)$ and $b^n(E)$ for $L = 32$, $\varepsilon = 2$, and $n_s = 5 \times 10^4$ entries in the histogram at different stages of the recursion procedure: $n = 100$ in Figures (a) and (b); $n = 400$ in Figures (c) and (d). For energies close to E_{GS}, $b(E)$ presents the expected noisy behavior because of the large fluctuations in the energy histogram.

energy bins. The tests for different energy bins were performed with a smaller number of sweeps $n_s = 2 \times 10^4$. Naturally, the number of recursion steps had to be further increased for this new setup. Again, the estimates for $b(E)$ are noisy. Moreover, ε produces strong changes on the behavior of $b(E)$. Unfortunately, a definite trend in the peak formation as a function of ε could not be seen. These figures show that the result $E/N \sim -1.14$ is obtained for the the intermediary value of $\varepsilon = 1$.

The situation is worse for $L = 56$ (data not shown), because after 800 recursion steps with $n_s = 2 \times 10^4$ the recursion procedure does not sample energies $E/N \lesssim -1.17$ properly, and up to the 999th recursion step there is no improvement for any tested bin ($\varepsilon = 0.8$, 1 and 1.2).

Now, for comparative purposes, Figure 4 brings the multicanonical and the Metropolis estimates of the average energy per spin E/N and canonical specific heat C_V as a function of canonical temperature T for $L = 32$. The Metropolis results were determined from multiple energy histograms. This approach consists of producing energy time series at different temperatures by means of the usual Metropolis update. By using reweighting techniques, those time series were combined to produce final estimates for the specific heat and susceptibility, see [17] and references therein. The results for $L = 32$ were obtained at five different temperatures with 3.4×10^7 sweeps in each histogram. The temperatures were chosen around the expected maxima of the specific heat. The multicanonical results are calculated from data exhibited in Figure 1 for $N_r = 400$ and further $n_{meas} = 6 \times 10^7$ sweeps.

The determination of the phase transition order requires reliable results for larger lattice sizes. Unfortunately, the standard multicanonical update does not sample conformations properly even for lattice sizes as small as $L = 32$. We have doubled

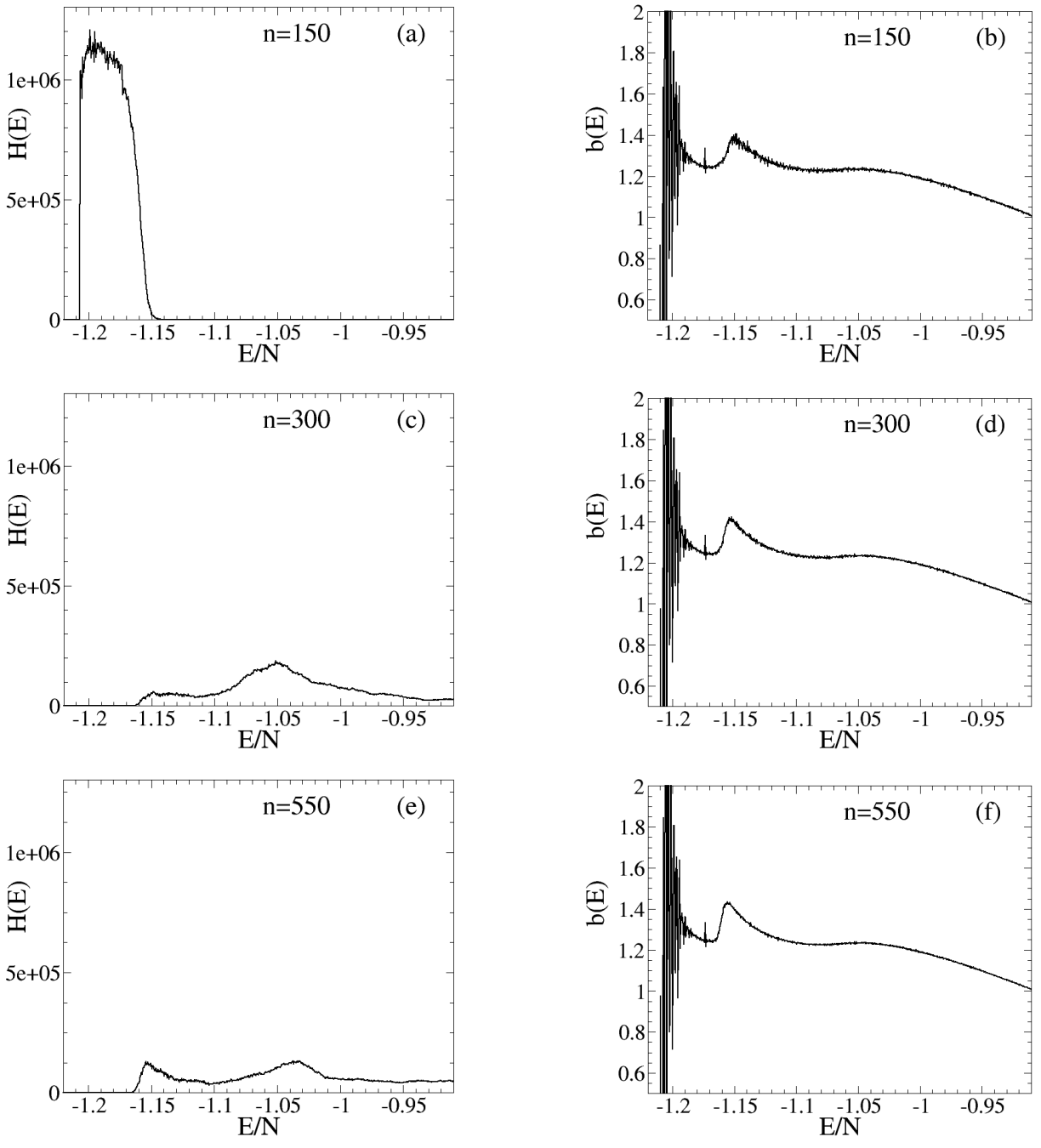

Figure 2 – Behavior of $H_{mu}^{n-1}(E)$ and $b^n(E)$ for $L = 48$, $\varepsilon = 1$, and $n_s = 5 \times 10^4$ entries in the histogram at three different stages of the recursion procedure: $n = 150$ in Figures (a) and (b); $n = 300$ in Figures (c) and (d); $n = 550$ in Figures (e) and (f).

the number of sweeps to update each histogram for $L = 48$ and 56, but the results remain essentially the same. The observed lack of tunneling events between two extremal energies means that it is required longer iterative runs, mainly as the system size increases. This of course, limits the applicability of the MUCA to this system.

4 CONCLUSIONS

In this study, the overall sampling performance of the MUCA for different energy bins and lattice sizes was compared in a model that describes ultrathin magnetic films and presents two free-energy barriers for the coupling $\delta = 2$. The intermediate

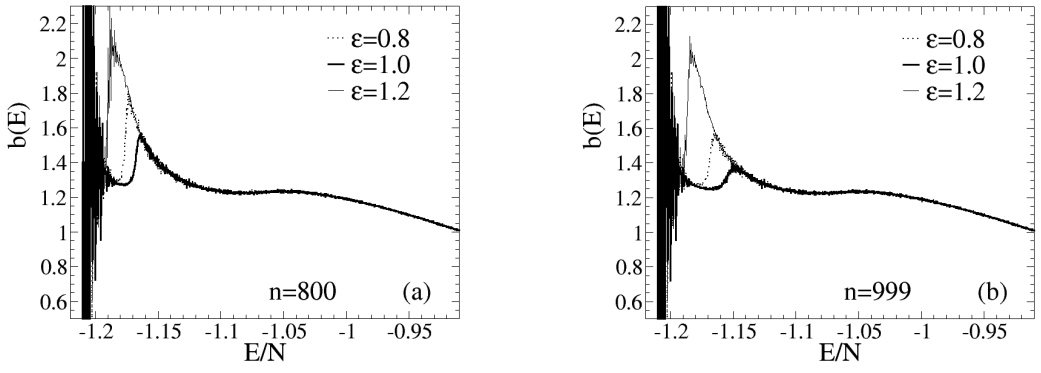

Figure 3 – Convergence of the multicanonical parameter $b(E)$ for $L = 48$, and $n_s = 2 \times 10^4$ entries in the histograms for different energy bins ε. Figure (a) shows results for $n = 800$ recursion steps, and (b) for $n = 999$.

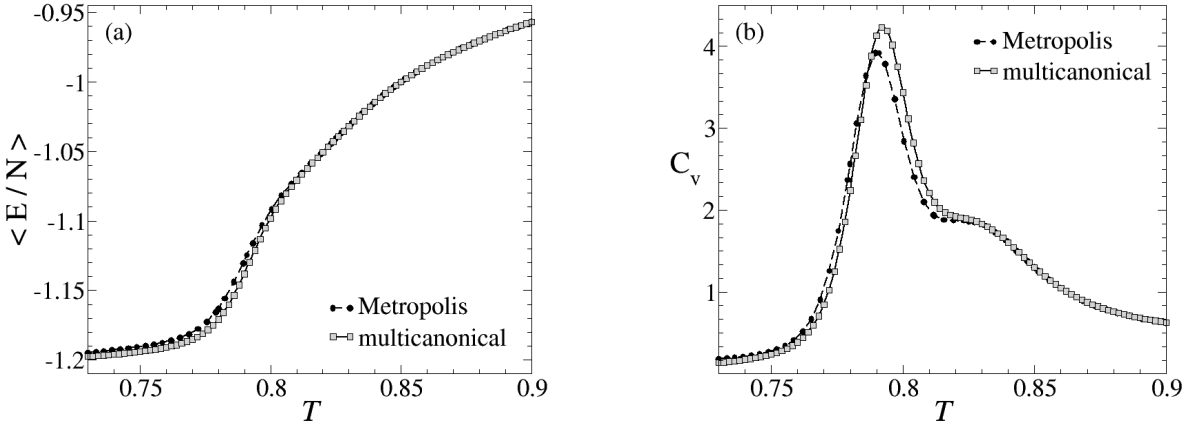

Figure 4 – Comparison between thermodynamic properties (a) energy per spin E/N and (b) canonical specific heat C_V as a function of the canonical temperature T obtained by reweighting Metropolis and multicanonical data for $L = 32$ and $\varepsilon = 2$.

results from different stages of the recursion procedure to obtain the multicanonical parameters are illustrated.

The sequence of phase transitions observed for this coupling is striped-nematic and, nematic-tetragonal at higher temperatures. Many studies based on local update algorithms have tried to infer the nature of those thermodynamic phase transitions. Since, the model is characterized by local minima that are separated by entropic barriers, we would expect that a generalized ensemble algorithm like MUCA would perform better in accelerating the convergence of our simulations. Although the generalized ensemble algorithms are efficient to sample configurations, it is known that all algorithms present limited success for systems with rugged free-energy landscapes. Unfortunately, this model with coupling $\delta = 2$, do not exhibit a satisfactory number of tunneling events even for a small lattice size as $L = 32$. This may result in misleading conclusions about the critical behavior because the multicanonical parameters could not be well evaluated, see our Figure 3. This difficulty in sampling configurations in a spin system is not exclusive to the 2D Ising model with dipole interactions. This was also observed in the implementation of another equivalent flat histogram algorithm for the modified XY model [25].

We remark that the suppression of tunneling events do not occur for smaller values of the coupling δ. In fact, a large number of tunneling events is observed for $\delta \in [0.89, 1.30]$, even for lattice sizes as large as $L = 72$ [26]. Thus, the critical behavior of this specific spin model with dipolar interactions for $\delta = 2$ becomes a challenge and should be considered a benchmark to test the performance of optimized MC algorithms.

ACKNOWLEDGMENTS

The authors acknowledge financial support from CNPq and FAPESP (Brazil).

REFERENCES

[1] LANDAU DP & BINDER K. 2000. A guide to Monte Carlo simulations in Statistics Physics. Cambridge University Press.

[2] SWENDSEN RH & WANG J-S. 1987. Nonuniversal critical dynamics in Monte Carlo simulations. Phys. Rev. Lett., 58: 86–88.

[3] KANDEL D, DOMANY E & BRANDT A. 1989. Simulations without critical slowing down: Ising and three-state Potts model. Phys. Rev. B, 40: 330–344.

[4] SALAS J & SOKAL AD. 1997. Dynamic critical behavior of the Swendsen-Wang algorithm: the two-dimensional three-state Potts model revisited. J. Stat. Phys., 87: 1–36.

[5] MITSUTAKE A, SUGITA Y & OKAMOTO Y. 2001. Generalized-ensemble algorithms for molecular simulations of biopolymers. Biopolymers, 60: 96–123.

[6] BERG BA & CELIK T. 1992. New approach to spin-glass simulations. Phys. Rev. Lett. 69: 2292–2295.

[7] BERG BA, HANSMANN U & CELIK T. 1994. Ground-state properties of the three-dimensional Ising spin glass. Phys. Rev. B, 50: 16444–16452.

[8] GROSSMANN B, LAURSEN ML, TRAPPENBEG T & WIESE UJ. 1992. A multicanonical algorithm for $SU(3)$ pure gauge theory. Phys. Lett. B, 293: 175–180.

[9] GROSSMANN B & LAURSEN ML. 1993. The confined-deconfined interface tension in quenched QCD using the histogram method. Nucl. Phys. B, 408: 637–656.

[10] SCHNABEL S, JANKE W & BACHMANN M. 2011. Advanced multicanonical Monte Carlo methods for efficient simulations of nucleation processes of polymers. J. Comp. Biol., 230: 4454–4465.

[11] DE'BELL K, MacISAAC AB & WHITEHEAD JP. 2000. Dipolar effects in magnetic thin films and quasi-two-dimensional systems. Rev. Mod. Phys., 72: 225–257.

[12] PORTMANN O, VATERLAUS A & PESCIA D. 2006. An inverse transition of magnetic domain patterns in ultrathin films. Nature, 422: 701–704; Observation of stripe mobility in a dipolar frustrated ferromagnet. Phys. Rev. Lett., 96: 047212 (2006).

[13] PÍGHIN S & CANNAS SA. 2007. Phase diagram of an Ising model for ultrathin magnetic films: Comparing mean field and Monte Carlo predictions. Phys. Rev. B, 75: 224433.

[14] BOOTH I, MacISAAC AB, WHITEHEAD JP & DE'BELL K. 1995. Domain structures in ultrathin magnetic films. Phys. Rev. Lett., 75: 950–953.

[15] ARLETT J, WHITEHEAD JP, MacISAAC AB & DE'BELL K. 1996. Phase diagram for the striped phase in the two-dimensional dipolar Ising model. Phys. Rev. B, 54: 3394–3402.

[16] CANNAS SA, MICHELON MF, STARIOLO DA & TAMARIT FA. 2006. Ising nematic phase in ultrathin magnetic films: A Monte Carlo study. Phys. Rev. B, 73: 184425.

[17] RIZZI LG & ALVES NA. 2010. Phase transitions and autocorrelation times in two-dimensional Ising model with dipole interactions. Physica B, 405: 1571–1579.

[18] CANNAS SA, MICHELON MF, STARIOLO DA & TAMARIT FA. 2008. Interplay between coarsening and nucleation in an Ising model with dipolar interactions. Phys. Rev. B, 78: 051602.

[19] BERG BA & NEUHAUS T. 1991. Multicanonical algorithms for first order phase transitions. Phys. Lett. B, 267: 249–253.

[20] BERG BA. 2000. Introduction to multicanonical Monte Carlo simulations. Fields Inst. Commun., 26: 1–24.

[21] BERG BA. 2003. Multicanonical simulations step by step. Comp. Phys. Comm., 153: 397–406.

[22] TOUKMAJI AY & BOARD Jr JA. 1996. Ewald summation techniques in perspective: a survey. Comput. Phys. Commun., 95: 73–92; GAO GT, ZENG XC & WANG W, 1996. Vapor-liquid coexistence of quasi-two-dimensional Stockmayer fluids. J. Chem. Phys., 106: 3311–3317.

[23] RASTELLI E, REGINA S & TASSI A. 2007. Phase diagram of a square Ising model with exchange and dipole interactions: Monte Carlo simulations. Phys. Rev. B, 76: 054438.

[24] GROSS DHE. 2001. Microcanonical thermodynamics: phase transitions in "small systems". World Scientific Publishing.

[25] SINHA S & ROY SK. 2009. Performance of Wang-Landau algorithm in continuous spin models and a case study: modified XY-model. Phys. Lett. A, 373: 308–314; 2010. Finite size scaling and first-order phase transition in a modified XY model. Phys. Rev. E, 81: 022102.

[26] FONSECA JSM, RIZZI LG & ALVES NA. (Unpublished).